Domain−Domain Communication for tRNA Aminoacylation: The Importance of Covalent Connectivity†

Chun-Mei Zhang and Ya-Ming Hou*

Department of Biochemistry and Molecular Pharmacology, Thomas Jefferson University, 233 South 10th Street, BLSB 220, Philadelphia, Pennsylvania 19107

Received February 16, 2005; Revised Manuscript Received April 4, 2005

ABSTRACT: Aminoacyl-tRNA synthetases form complexes with tRNA to catalyze transfer of activated amino acids to the 3′ end of tRNA. The tRNA synthetase complexes are roughly divided into the activation and tRNA-binding domains of synthetases, which interact with the acceptor and anticodon ends of tRNAs, respectively. Efficient aminoacylation of tRNA by *Escherichia coli* cysteinyl-tRNA synthetase (CysRS) requires both domains, although the pathways for the long-range domain−domain communication are not well understood. Previous studies show that dissection of $tRNA^{Cys}$ into acceptor and anticodon helices seriously reduces the efficiency of aminoacylation, suggesting that communication requires covalent continuity of the tRNA backbone. Here we tested if communication requires the continuity of the synthetase backbone. Two N-terminal fragments and one C-terminal fragment of *E. coli* CysRS were generated. While the N-terminal fragments were active in adenylate synthesis, they were severely defective in the catalytic efficiency and specificity of tRNA aminoacylation. Conversely, although the C-terminal fragment was not catalytically active, it was able to bind and discriminate tRNA. However, addition of the C-terminal fragment to an N-terminal fragment in trans did not improve the aminoacylation efficiency of the N-terminal fragment to the level of the full-length enzyme. These results emphasize the importance of covalent continuity of both CysRS and $tRNA^{Cys}$ for efficient tRNA aminoacylation, and highlight the energetic costs of constraining the tRNA synthetase complex for domain−domain communication. Importantly, this study also provides new insights into the existence of several natural "split" synthetases that are now identified from genomic sequencing projects.

Aminoacyl-tRNA synthetases (aaRSs) are modular enzymes that arose early to interpret the genetic code. These enzymes catalyze aminoacylation of tRNAs to relate amino acids to the anticodon trinucleotide sequences. The overall architecture of tRNA synthetases consists of primarily two domains (*1*). The active site domain is responsible for activation of an amino acid with ATP in synthesizing an enzyme-bound aminoacyl-adenylate, and transfer of the aminoacyl-adenylate intermediate to the 3′ end of tRNA. The second domain is responsible for selection and binding of the cognate tRNA. In the course of evolution, appended domains have been added to the two-domain structure to perform other functions. For example, some synthetases have an editing domain that hydrolyzes misacylated amino acids that are not sufficiently distinguished by the active site domain (*1*).

The two-domain structure of synthetases parallels the two-domain structure of the L-shaped tRNA (*2*). In high-resolution crystal structures of tRNA synthetase complexes, the active site domain of synthetases interacts with the tRNA acceptor-T helix, while the second domain contacts the anticodon. Efficient aminoacylation of tRNA for most synthetases requires communication between the two domains (reviewed in ref *3*). This is clearly demonstrated by mutational effects on steady-state kinetics of aminoacylation. For example, mutations of tRNA anticodon triplets, or of residues in the anticodon-binding domain of synthetases, often lead to severely reduced catalytic efficiency of aminoacylation. The driving force in these reductions is usually a decrease in k_{cat} by several orders of magnitude (*4*). Thus, the signal of improper contact at the anticodon end is communicated to the active site to affect the k_{cat} of aminoacylation.

The mechanism of domain−domain communication is not well understood. Earlier studies have shown that the communication is interrupted when the tRNA backbone is broken, based on observations that truncated tRNA molecules consisting of just the acceptor helix have extremely poor efficiencies of aminoacylation (*5*, *6*), and that the poor efficiencies cannot be improved even with addition of the corresponding anticodon helix (*7*, *8*). These studies have revealed high costs of thermodynamic energy required for communication between the two domains of tRNA (*9*). The requirement for the protein covalent backbone is less clear. Proteins such as ribonuclease A (*10*) have been split and re-assembled noncovalently to reconstitute their activities. Conceivably, protein enzymes are larger than tRNAs and thus have higher-order packing capacities that may use

† This work was supported by Grant GM56662 from the National Institutes of Health (to Y.-M.H.). C.-M.Z. is the recipient of a postdoctoral fellowship of American Heart Association-Pennsylvania Division.

* To whom correspondence should be addressed. Phone: (215) 503-4480. Fax: (215) 503-4954. E-mail: Ya-Ming.Hou@jefferson.edu.

10.1021/bi050285y CCC: $30.25
Published on Web 04/23/2005

subunit interfaces to mediate molecular signaling. Additionally, through their extensive contact surfaces with tRNA, synthetases may use intermolecular contacts to provide pathways for communication. Indeed, genetic analysis has shown that certain bacterial synthetases can be created in pieces and re-assembled in vivo to function in aminoacylation (*11*−*13*). Most intriguingly, various genomic sequencing projects have identified naturally split synthetase genes (*14*, *15*) or genes that encode free-standing domains of synthetases (*16*−*18*). These have raised the possibility that split genes can be expressed separately to form subunits of a functional enzyme. Although the implication of split genes is that functional synthetases can be created without a covalently connected backbone, the energetic costs of domain−domain communication in such cases are not known.

To gain insights into the concept of split genes, its general applicability, and energetic costs, we artificially separated a synthetase into two domains and tested their ability to maintain domain−domain communication. We used *Escherichia coli* CysRS[1] as an example, which is the smallest monomer of the class I synthetases (461 amino acids) and can be easily defined by the two-domain structure (*19*). Efficient aminoacylation by CysRS requires communication between the active site domain at the N-terminus and the tRNA-binding domain at the C-terminus. This is based on the 10^3−10^4 fold reduction in the efficiency of aminoacylation upon mutations of the tRNA anticodon (*20*), and on the 10^5-fold reduction upon removal of the anticodon helix, leaving just the mini- and microhelices of the acceptor stem (*21*). Although the acceptor helices contain the most important nucleotide, U73, for aminoacylation (*20*, *22*), their poor efficiency cannot be rescued by the addition of the anticodon helix (*21*). This clearly suggests the requirement of the covalent connectivity of the tRNA backbone, and sets the stage for addressing the converse experiment in CysRS. Importantly, the crystal structure of the enzyme in complex with $tRNA^{Cys}$ has recently been determined (*23*), which provides a valuable framework for designing and interpreting experiments. Here we report dissection of *E. coli* CysRS into the N- and C-domains and their ability to function separately and together in trans. Additionally, we seek to obtain both kinetic and thermodynamic parameters of the two domains for aminoacylation of $tRNA^{Cys}$, to gain insights into the energetic costs required for domain−domain communication.

MATERIALS AND METHODS

Construction of Deletion Fragments of E. coli CysRS. The pCysRS09 plasmid (a derivative of pET-22b) (*24*), containing the wild-type sequence of *E. coli* CysRS inserted between the *Nde*I and *Bam*HI restriction sites, was used as the template for construction of deletion fragments. Introduction of a second *Bam*HI site, and restriction of the resulting plasmids with *Bam*HI, followed by religation, created the reading frame for the N-terminal fragments. The reading frame for the C-terminal fragment ($C_{277-461}$) was created by introducing the start codon (AUG) to position 276. All mutations were achieved by QuikChange mutagenesis (Stratagene). Screening for mutant genes was achieved by direct sequencing at the Jefferson core facility. Mutations were obtained at 75−100% efficiency.

Enzyme Purification. The full-length *E. coli* $CysRS_{1-461}$, harboring a C-terminal His tag, was expressed from pCysRS09 in *E. coli* BL21(DE3) cells. A half liter of cells was grown in LB/Amp and induced with 0.4 mM IPTG for 3−5 h at 37 °C. The cell paste was resuspended in 10 mL of sonication buffer [20 mM Tris-HCl (pH 8.0), 100 mM NaCl, and 5 mM β-mercaptoethanol], sonicated for 5 × 15 s, and centrifuged at 15 000 rpm for 30 min to obtain the cleared cell lysate. The overexpressed CysRS, which represented more than 90% of total soluble cellular proteins, was purified from the cell lysate by incubation with 2 mL of the His-link resin (Promega) equilibrated in the sonication buffer for 30 min at 4 °C. The resin was washed five times with the sonication buffer and 10 mM imidazole before CysRS was eluted with 100 mM imidazole. The purified CysRS was near 99% homogeneity, as judged from SDS−PAGE, and used directly for assays. The soluble fractions of N_{1-287}, N_{1-327}, and $C_{277-461}$ fragments of CysRS were purified by the same general protocol. The protein concentrations of the full-length and deletion mutants of CysRS were determined by the Bradford method, while the enzyme concentrations of the full-length and N-terminal fragments were determined by the active site burst assay (*25*).

Preparation of $tRNA^{Cys}$ and $Microhelix^{Cys}$. The full-length *E. coli* $tRNA^{Cys}$ was prepared by runoff transcription of the *Bst*NI-linearized pTFMa-Cys01 by T7 RNA polymerase as described previously (*26*). The transcript was purified from a 12% PAGE/7 M urea gel, crushed and soaked in TE [10 mM Tris-HCl (pH 8.0) and 1 mM EDTA], and recovered by ethanol precipitation. The concentration of the tRNA transcript was estimated by the absorption at A_{260} (1 OD = 40 mg/L) and corrected by plateau charging. Microhelices of $tRNA^{Cys}$ were chemically synthesized by Dharmacon (Boulder, CO), deprotected, and resuspended in TE prior to use. The concentrations of microhelices were determined by the absorption at A_{260}.

ATP−PP_i Exchange Assay. The previously established ATP−PP_i exchange assay (*27*) was modified by using [γ-^{32}P]ATP as the substrate, rather than [^{32}P]PP_i. The reaction mixture contained 0.1 M Tris-HCl (pH 8.0), 2 mM $NaPP_i$, 10 mM β-mercaptoethanol, 0.1 mg/mL BSA, 0.1 mM EDTA, 10 mM KF, 5 mM $MgCl_2$, 500 mM cysteine, and varying concentrations of [γ-^{32}P]ATP (5 × 10^6 cpm/mmol). With the addition of 50 nM enzyme, the reaction mixture was incubated at room temperature and 50 μL aliquots were removed at defined time points and quenched with 20 μL of 24% perchloric acid and 50 μL of rapidly stirring charcoal suspension (3% acid-washed charcoal in 0.5% HCl). The quenched reaction mixture was spun at 15 000 rpm for 10 min, and an aliquot of the [^{32}P]PP_i released into the charcoal-free supernatant was counted by a scintillation counter.

Aminoacylation Assay. Aminoacylation of $tRNA^{Cys}$ or $microhelix^{Cys}$ with [^{35}S]cysteine (12 000 dpm/pmol) was as described previously (*28*, *29*). Reactions were performed at 37 °C, and aliquots were removed at various time points, quenched by carboxymethylation, and precipitated on a filter pad in 5% trichloroacetic acid. The concentrations of tRNA were determined from plateau charging.

[1] Abbreviations: CysRS, cysteinyl-tRNA synthetase; HisRS, histidyl-tRNA synthetase; ProRS, prolyl-tRNA synthetase; LeuRS, leucyl-tRNA synthetase; AlaRS, alanyl-tRNA synthetase; DTT, dithiothreitol; PAGE, polyacrylamide gel electrophoresis.

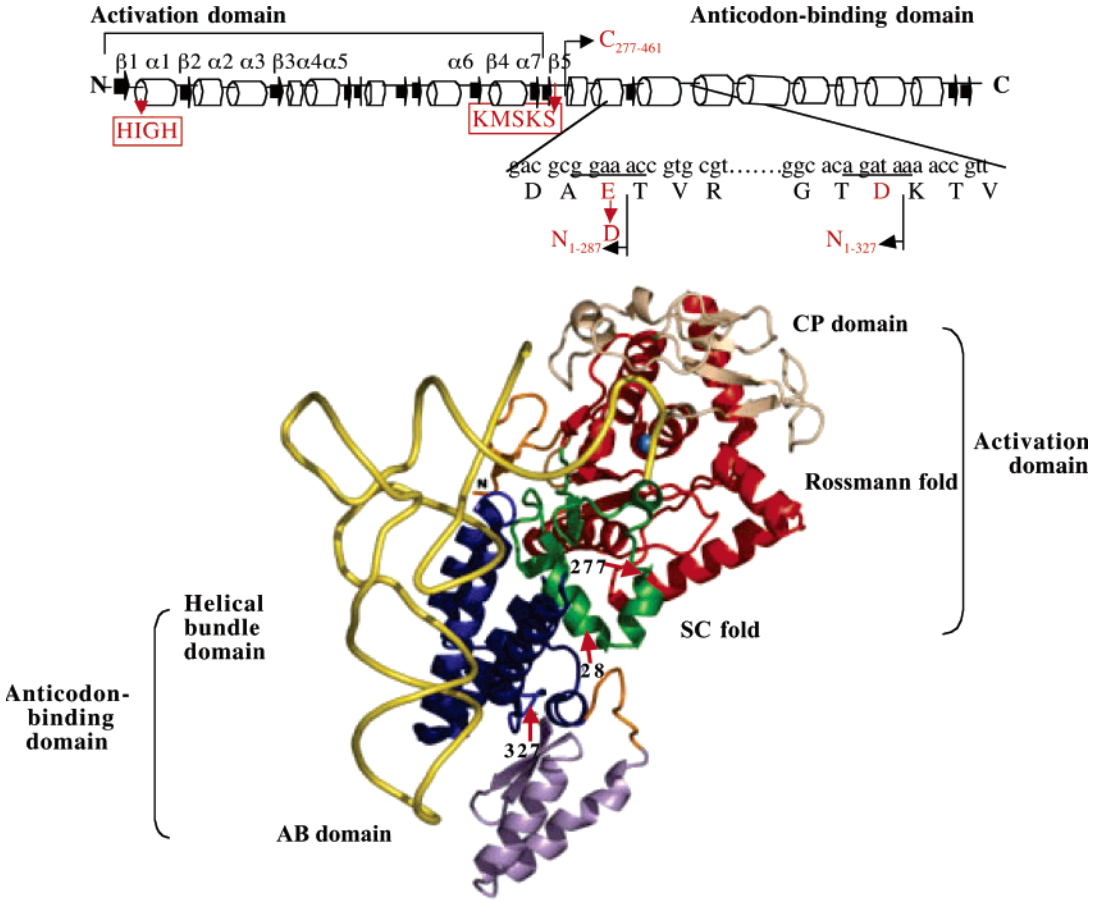

FIGURE 1: Secondary structure diagram (top) and crystal structure of the *E. coli* CysRS−tRNA^{Cys} complex (bottom). In the secondary structure diagram, helices are represented by cylinders and β-strands by arrows. The HIGH and KMSKS motifs are represented by boxes, while mutations in the SC fold for generating the reading frames of N_{1-287}, N_{1-327}, and $C_{277-461}$ fragments are colored red. In the crystal structure of the complex, the Rossmann fold and CP domain in the active site domain are colored red and light brown, respectively. The anticodon-binding domain consists of the helical bundle domain (dark blue) and the AB domain (purple). The SC fold (green) joins the activation domain with the anticodon-binding domain.

Fluorescence Measurement of Binding tRNA^{Cys}. Equilibrium fluorescence binding titration of tRNA^{Cys} was carried out at room temperature with 0.05−0.25 μM enzyme in 20 mM Tris-HCl (pH 7.5), 50 mM NaCl, and 5 mM β-mercaptoethanol or in 50 mM HEPES (pH 7.5) and 10 mM $MgCl_2$. The intrinsic tryptophan titration was excited at 285 nm, and the emission was monitored from 300 to 400 nm. An emission wavelength of 330 nm was used to quantify binding after correction of dilution. Controls with BSA or tryptophan showed no fluorescence response to tRNA. The fluorescence change in response to tRNA concentration was fitted to a hyperbolic binding curve.

Complementation Assay. The *E. coli* chromosomal *cysS* deletion strain, constructed previously by disrupting the gene with a chloramphenicol marker (*30*), was used as the test strain. This deletion strain harbors the intact but arabinose-controllable *Haemophilus influenzae cysS* gene integrated into the CRIM recombination sites. To express the synthetase-encoding pET-22b plasmids, the T7 RNA polymerase gene, λDE3, was integrated into the chromosome using the λDE3 lysogenization kit (Novagen). The pET-22b derivative plasmids encoding sequences for the N_{1-287} and N_{1-327} fragments were introduced into the *cysS*$^-$ strain by transformation and selected for ampicillin resistance. Transformants were tested for complementation by streaking them on an LB/Amp plate supplemented with IPTG in the absence of 1 mM arabinose at 37 °C.

RESULTS

Construction of the N- and C-Terminal Fragments of E. coli CysRS. According to crystal structures of the enzyme (*23*, *31*), the active site domain of the Rossmann fold is located at the N-terminus and begins with the β_1 sheet and continues with the pattern of alternating α and β until β_5. The class I-specific HIGH sequence (at positions 37−40) is at the beginning of α_1, while the other class I-specific KMSKS sequence (at positions 266−270) is located after β_5 in a flexible loop, known as the SC fold (stem−contact fold), that directly connects the Rossmann fold with the C-terminal anticodon-binding domain (Figure 1). The SC fold is near the inside corner of the tRNA L shape, and is responsible for global positioning of the tRNA on the enzyme surface. The importance of the SC fold in connecting the N- and C-terminal domains, and its proximity to the tRNA tertiary core, provided the rationale for introducing truncation sites into this region. One truncation site was chosen at E287, which is not in direct contact with the tRNA core, to minimize alteration of enzyme−tRNA contact areas upon truncation. E287 is in a solvent-accessible position within an α-helix of the SC fold that completes the turn of the

KMSKS-containing loop. Another truncation site was chosen after D327, which is near the end of the SC fold and is also a solvent-accessible residue. As shown below, because the N-terminal fragment that ended at E287 (N_{1-287}) was more active than the one that ended at D327 (N_{1-327}), the C-terminal complementing fragment was designed to begin at V277 ($C_{277-461}$), which precedes the α-helix that contained E287. In this design, the α-helix that is broken by E287 in the N_{1-287} fragment is kept intact in the overlapping C-terminal fragment.

To generate the CysRS fragments, the wild-type pCysRS09 plasmid, containing the *cysS* gene between the *Nde*I and *Bam*HI sites of pET-22b, was used as the template. Expression of the wild-type plasmid yielded the full-length enzyme with a C-terminal His tag ($CysRS_{1-461}$), where the tag has been shown to have no effect on the catalytic activity of the synthetase (*24*). The reading frames for the N_{1-287} and N_{1-327} fragments were created by generating a second *Bam*HI site after the desired codons, followed by cleavage of the resulting plasmids with *Bam*HI and rejoining. As a result of the second *Bam*HI site, the E287 residue in the N_{1-287} fragment was changed to D287 (Figure 1). The reading frame for the $C_{277-461}$ fragment was created by introducing a second *Nde*I site at position 276, followed by cleavage of the resulting plasmid with *Nde*I and rejoining between the existing and engineered *Nde*I sites. All three reading frames maintained the sequence for the C-terminal His tag.

Although all three fragments were abundantly expressed in *E. coli*, the two N-terminal fragments were largely precipitated in inclusion bodies. Despite considerable efforts to explore and test different growth conditions, these two fragments remained insoluble. The solubility problem is not necessarily the result of the arbitrary truncation, because a naturally occurring N-terminal fragment of CysRS is also insoluble under similar laboratory conditions. This protein is MshC of *Mycobacteria* species, which synthesizes cysteinyl-adenylate in a pathway leading to the biosynthesis of mycothiol (*32*). In *Mycobacteria* species, mycothiol is the major reducing agent that protects these bacteria against oxidative stress. Because of the insolubility problem, the small soluble fraction of the two N-terminal fragments was used for protein purification, which was achieved by binding these fragments to a metal affinity resin under native conditions and eluting them with imidazole. The concentrations of these N-terminal fragments were determined by the active site burst assay (*25*). In contrast, the $C_{277-461}$ fragment was soluble and was readily purified to homogeneity. The concentration of this fragment was determined on the basis of protein quantities.

The N-Terminal Fragments Functioned in Synthesis of Cysteinyl Adenylate. The integrity of the N_{1-287} and N_{1-327} fragments was assessed by their ability to activate cysteine with ATP to generate cysteinyl-AMP. This activity was assayed by the ATP−PP_i exchange reaction, where [γ-^{32}P]ATP was the substrate and the forward synthesis of [^{32}P]PP_i was monitored. In the presence of a saturating level of cysteine (500 μM), the rate of exchange was measured under steady-state conditions. For the full-length $CysRS_{1-461}$, the K_m for ATP was 0.25 mM (Table 1), which was the same as the published K_m obtained from the reverse reaction using [^{32}P]PP_i as the substrate (*27*). However, the k_{cat} of the forward reaction was 22.6 s^{-1} for $CysRS_{1-461}$, which was ∼6-fold below that of the reverse reaction (k_{cat} = 142 s^{-1}). The slower k_{cat} of the forward reaction might result from contaminating nonhydrolyzable compounds in [γ-^{32}P]ATP or from contaminating ATPase in the protein sample. Alternatively, it might reflect a fundamental difference between the forward and reverse reactions.

Table 1: ATP−PP_i Exchange Kinetics[a]

	K_m (mM)	k_{cat} (s^{-1})	k_{cat}/K_m (M^{-1} s^{-1})	relative
$CysRS_{1-461}$	0.25 ± 0.002	22.6 ± 2.3	9.0×10^4	1.0
N_{1-287}	0.31 ± 0.04	2.0 ± 0.1	6.4×10^3	0.07
N_{1-327}	1.18 ± 0.08	0.34 ± 0.06	2.9×10^2	3.2×10^{-3}

[a] $CysRS_{1-461}$ (at 50 nM) and N_{1-287} (at 200 nM) were assayed over a range of ATP concentrations from 0.05 to 2 mM, while N_{1-327} (at 500 nM) was assayed over a range of ATP concentrations from 0.1 to 5 mM.

Both the N_{1-287} and N_{1-327} fragments were active in the synthesis of cysteinyl adenylate in the ATP−PP_i exchange assay, albeit with a lower efficiency than the full-length $CysRS_{1-461}$ (Table 1). Of the two, the N_{1-287} fragment was more active, with a K_m for ATP closely similar to that of the full-length protein (0.31 mM) but a k_{cat} decreased by 10-fold (2 s^{-1}). This resulted in a catalytic efficiency (k_{cat}/K_m) approximately 10-fold reduced from that of the full-length protein. The N_{1-327} fragment showed a significant increase in K_m for ATP by 5-fold to 1.18 mM and a further 10-fold decrease in k_{cat} to 0.34 s^{-1}, yielding a k_{cat}/K_m more than 300-fold reduced from that of the full-length CysRS. The weaker activity of the N_{1-327} fragment was unexpected because this fragment contains nearly the complete sequence of the SC fold. Possibly, the longer N_{1-327} fragment folds less well than the shorter N_{1-287} fragment, and the presence of a C-terminal His tag further impedes proper folding. The folding problem is likely due to the absence of the C-terminal domain, where the SC fold might adopt a misfolded structure, such that the preceding KMSKS sequence is prevented from aligning for adenylate synthesis. The notion of misalignment is consistent with the k_{cat} defect being more pronounced than the K_m defect in both N-terminal fragments. Of the two fragments, the more active N_{1-287} fragment was used in further analysis.

The N_{1-287} Fragment Functioned in Aminoacylation of the Microhelix of $tRNA^{Cys}$. In addition to catalyzing adenylate synthesis, the active site domain should also catalyze transfer of the activated aminoacyl group to the 3′ end of tRNA. With the active site domain using only the tRNA acceptor helix as the substrate, its catalytic efficiency should be comparable to that of the full-length synthetase, which would not have the advantage of binding to the tRNA anticodon. The kinetic competence of the N_{1-287} fragment was tested for its ability to catalyze cysteinylation of the microhelix of $tRNA^{Cys}$, lacking the entire T stem and the D anticodon sequence (Figure 2). $Microhelix^{Cys}$ was chemically synthesized on the basis of the sequence of the acceptor stem of $tRNA^{Cys}$, and contained the UUCG tetraloop to join the two sides of the stem. The aminoacylation activity of this microhelix has been previously established by the full-length $CysRS_{1-461}$, showing a rather high K_m (∼200 μM) and a low k_{cat} in the range of 10^{-4} s^{-1} (*29*). Because of the high K_m for $microhelix^{Cys}$, the kinetics of aminoacylation by the truncated N_{1-287} fragment was focused on the k_{cat}/K_m parameter only. At concentrations of $microhelix^{Cys}$ at least 40-fold below the K_m, the initial

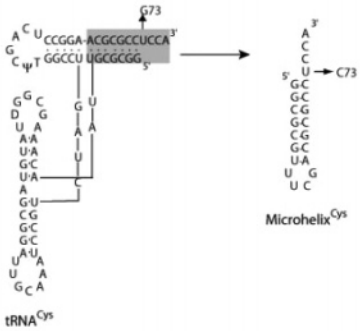

	$CysRS_{1-461}$ $k_{cat}/K_M(M^{-1}s^{-1})$	N_{1-287} $k_{cat}/K_M(M^{-1}s^{-1})$
U73microhelix^{Cys}	2.54 ± 0.06	2.3 ± 0.1
C73microhelix^{Cys}	-	-
A73microhelix^{Ala}	-	-
U73microhelix^{Ala}	1.0 ± 0.2	1.2 ± 0.4
U73tRNA^{Cys}	2.0 X 10^6	1.3 X 10^2
G73tRNA^{Cys}	2.6 ± 0.2	0.41 ± 0.01

FIGURE 2: Sequence and L-shaped arrangement of *E. coli* tRNA^{Cys}, where the microhelix^{Cys} domain is shaded. Mutations of U73 to G in tRNA^{Cys} or to C in the microhelix are indicated. The k_{cat}/K_m parameter of aminoacylation by $CysRS_{1-461}$ and by N_{1-289} is shown below.

rate of aminoacylation was measured and used as an approximation of k_{cat}/K_m. This value for full-length $CysRS_{1-461}$ was 2.54 M^{-1} s^{-1} (Figure 2), which was in good agreement with the previous study (*28*) and represented a 10^6-fold decrease from the k_{cat}/K_m of aminoacylation of full-length tRNA^{Cys} (2×10^6 M^{-1} s^{-1}). The k_{cat}/K_m value of the N_{1-287} fragment was virtually identical (2.3 M^{-1} s^{-1}) to that of full-length $CysRS_{1-461}$. This was interesting, given that the N_{1-287} fragment is deficient in adenylate synthesis by 10-fold (Table 1). Possibly, the perturbation of the active site in the N_{1-287} fragment that caused the 10-fold reduction in the efficiency of adenylate synthesis was partially repaired by the presence of the microhelix, as previously suggested in aminoacylation of full-length tRNA (*27*).

The specificity of aminoacylation of microhelix^{Cys} was examined for the N_{1-287} fragment (Figure 2). The most important nucleotide for aminoacylation in the microhelix and tRNA^{Cys} is U73 (*20*, *21*). Both this fragment and the full-length $CysRS_{1-461}$ lost their aminoacylation activity upon substitution of U73 with C, indicating a strong dependence on U73 for aminoacylation. To further test the specificity, U73 was introduced into the microhelix of tRNA^{Ala} to create the U73 variant of microhelix^{Ala}. Importantly, while the normal A73-containing microhelix^{Ala} was not a substrate for cysteinylation by the full-length protein or the N_{1-287} fragment, the U73 variant was a substrate for both. The catalytic efficiency of aminoacylation of the U73 microhelix^{Ala} by the full-length $CysRS_{1-461}$ and the N_{1-287} fragment was nearly identical, suggesting that the fragment has completely recapitulated the activity and specificity of the full-length enzyme in aminoacylating tRNA acceptor helices.

The N_{1-287} Fragment Supported Cell Growth. The ability and specificity of the N_{1-287} fragment to aminoacylate microhelix^{Cys} raised the possibility that it might aminoacylate the larger and anticodon-containing tRNA^{Cys} so that this activity would be sufficient to support cell growth. The cellular activity demands that the fragment only recognize cysteine and transfer it to tRNA^{Cys}, but to no other tRNAs. A previously constructed *E. coli* strain, containing a disrupted *cysS* gene, was used to test this possibility (*30*). Because the *cysS* gene is essential for *E. coli* growth, the *cysS*$^-$ strain was maintained by introducing the highly homologous *H. influenzae cysS* gene into the *E. coli* chromosome under the control of the arabinose promoter. In growth media lacking arabinose, the viability of the *cysS*$^-$ strain would depend on a functional synthetase that can aminoacylate tRNA^{Cys} with cysteine. When this *cysS*$^-$ strain was supplied with the plasmid-borne full-length $CysRS_{1-461}$, expressed from the strong and inducible *lac* promoter, it was viable and displayed a robust growth phenotype, indicating rescue of the *cysS*$^-$ gene.

Table 2: Growth Complementation of the *E. coli cysS*$^-$ Strain[a]

CysRS	k_{cat}/K_m of aminoacylation of tRNA^{Cys} in vitro (relative)	growth complementation (relative growth)
$CysRS_{1-461}$	1.0	+++++
C28S	1.2×10^{-4}	+
C209S	3.1×10^{-5}	−
C28S/C209S	2.6×10^{-5}	−
H234S	1.5×10^{-4}	−
E238S	0.3	++++
H234N/E238Q	5.9×10^{-5}	−
C28S/C209S/H234N/E238Q	not detectable	−
H206S	0.6	+++++
H224S	5.7×10^{-2}	++
H235S	3.8×10^{-3}	+++
H224N/H235N	4.2×10^{-4}	++
H256S	0.1	++
H234N/E238Q/H224N/H235N	not detectable	−
W205F	5.5×10^{-3}	+++
N351D	2.5×10^{-3}	++++
E354Q	0.1	+++++
N_{1-287}	6.0×10^{-5}	++
N_{1-327}	not detectable	−

[a] Each CysRS enzyme (k_{cat}/K_m obtained from ref *27* or this study) was expressed in the *E. coli* cysS$^-$ strain on an LB/ampicillin/IPTG plate with or without 1 mM arabinose at 37 °C for 16 h. Growth was compared to the growth of the wild type on the basis of the number of cells and the strength of growth.

The N_{1-287} fragment and several previously characterized mutants of CysRS were tested for their ability to rescue the *cysS*$^-$ gene (Table 2). The selected mutants all contained substitutions at the active site, and their various mutations were intended to provide a range of different growth phenotypes. The active site of CysRS features an important zinc ion that is coordinated by four conserved residues (C28, C209, H234, and E238) (*24*), and is catalytically modulated by a layer of five conserved histidines (H206, H224, H234, H235, and H256) (*27*). The CysRS uses the zinc ion to select cysteine by establishing the strong and favorable zinc−thiolate bond that is not possible with any noncognate amino acids. After the zinc−thiolate bond has formed, a conserved W205 nearby is shifted into the active site to stabilize the bound cysteine. All of these key residues in the active site have been mutated, and these mutations caused varying deficiencies in aminoacylation of tRNA^{Cys} (*27*). In the rescue assay of the *cysS*$^-$ gene, mutants defective in the k_{cat}/K_m of aminoacylation of tRNA^{Cys} by less than 10-fold had the same robust growth phenotype as the wild type. Those defective by 10^2−10^4-fold exhibited progressively diminishing growth, while those defective by more than 10^4-fold showed no detectable growth. Notably, the N_{1-287} fragment showed weak but clear growth, while the less active N_{1-327} showed

Table 3: Aminoacylation of $tRNA^{Cys}$ Kinetics[a]

enzyme	K_m (μM)	k_{cat} (s^{-1})	k_{cat}/K_m (M^{-1} s^{-1})	relative
$CysRS_{1-461}$	1.16 ± 0.01	2.46 ± 0.06	2.1×10^6	1.0
N_{1-287}	~120		$(1.3 \pm 0.9) \times 10^2$	6.0×10^{-5}
$C_{277-461}$	not tested	not tested	not tested	
N_{1-287} and $C_{277-461}$	1.7 ± 0.6	$(3.9 \pm 0.04) \times 10^{-4}$	2.3×10^2	1.1×10^{-4}

[a] The kinetic parameters of full-length $CysRS_{1-461}$ were obtained from previously published results (*27*). The K_m of the N_{1-287} fragment was obtained by estimation, while the apparent k_{cat}/K_m was obtained by measuring the initial rate of aminoacylation at low tRNA concentrations (5−10 μM) and the fragment at 0.5 μM.

no complementation. The growth indicates rescue of the *cysS*$^-$ gene and suggests that, although the N_{1-287} fragment lacks the domain for binding the tRNA anticodon, its activity for the tRNA acceptor end is sufficiently strong and specific to support aminoacylation of $tRNA^{Cys}$ with cysteine in vivo.

In Vitro Aminoacylation of $tRNA^{Cys}$ by the N_{1-287} Fragment. To directly test aminoacylation of $tRNA^{Cys}$ by the N_{1-287} fragment, the kinetics of aminoacylation was measured in vitro. To ensure that aminoacylation was not due to contaminating activity of the endogenous CysRS, this fragment was purified through more stringent washes of the metal affinity resin, or alternatively purified from the *cysS*$^-$ strain under conditions where expression of the *H. influenzae cysS* gene was turned off. In the latter case, there was no endogenous full-length CysRS so that the growth ability of the *cysS*$^-$ strain was entirely dependent on the N_{1-287} fragment. The purified N_{1-287} fragments from both conditions were indeed active for aminoacylation of $tRNA^{Cys}$, and were similar in activity. Because the K_m for the N_{1-287} fragment for $tRNA^{Cys}$ was high (estimated to be ~120 μM), the kinetics was evaluated by the k_{cat}/K_m parameter under conditions where the tRNA substrate concentration was at least 20-fold below the K_m (Table 3). This analysis showed a k_{cat}/K_m of 1.3×10^2 M^{-1} s^{-1} by the N_{1-287} fragment, which is nearly 10^4-fold lower than that of the full-length CysRS and is consistent with the predicted range based on the rescue phenotype of the *cysS*$^-$ strain (Table 2).

The specificity of aminoacylation was addressed by testing mutations of U73 in $tRNA^{Cys}$, to allow comparison of the specificity between the N_{1-287} fragment and full-length CysRS (Figure 2). The G73 variant of $tRNA^{Cys}$ was prepared, and the k_{cat}/K_m parameter was determined. The N_{1-287} fragment was sensitive to the mutation and showed a nearly 300-fold reduction in k_{cat}/K_m (0.41 M^{-1} s^{-1}) compared to that of the U73 tRNA. Interestingly, while full-length $CysRS_{1-461}$ was also sensitive to the mutation, it showed a reduction in k_{cat}/K_m of almost 10^6-fold (2.6 vs 2.0×10^6 M^{-1} s^{-1}). Thus, the full-length CysRS gained additional specificity by simply containing the anticodon-binding domain.

The weak aminoacylation activity of the N_{1-287} fragment provided an opportunity to address whether addition of the anticodon-binding domain would restore aminoacylation in vitro to that of full-length CysRS. The $C_{277-461}$ fragment, containing the complete anticodon-binding domain and a significant portion of the SC fold, was incubated with the N_{1-287} fragment at a 1:1 molar ratio to allow the two fragments to reach a stable but noncovalently packed structure. The N_{1-287} fragment was then assayed for aminoacylation of $tRNA^{Cys}$ with cysteine (Table 3). Intriguingly, while the K_m for $tRNA^{Cys}$ (1.7 μM) was reduced from ~120 μM to almost the same as that of full-length $CysRS_{1-461}$ (1.0 μM), the k_{cat} remained severely defective by 10^4-fold.

Equilibrium K_d (μM) determined by fluorescence

Enzyme	$CysRS_{1-461}$	N_{1-287}	$C_{277-461}$
$U73tRNA_{GCA}$	0.33	9.5 ±1.1	0.33 ± 0.02
$U73tRNA_{CUA}$	5.2±0.7		3.7±0.5
$G73\ tRNA_{GCA}$	2.5±0.5	7.2±0.4	

FIGURE 3: Sequence and cloverleaf structure of *E. coli* $tRNA^{Cys}$, where mutations of U73 to G and mutations of the GCA anticodon to CUA are indicated. The equilibrium binding constant (K_d), determined by fluorescence titration, for various tRNA substrates is shown below.

Although the stable association of the two fragments could not be easily established by biochemical means, the almost wild-type K_m suggested the possibility that the mixture of the two fragments had nearly restored the kinetic binding affinity for full-length $tRNA^{Cys}$ as $CysRS_{1-461}$ during aminoacylation. However, the extremely weak k_{cat} suggested that the restored kinetic binding affinity was unable to facilitate catalysis, resulting in an overall k_{cat}/K_m still 10^4-fold below that of the full-length enzyme.

The $C_{277-461}$ Fragment Functioned in Binding and Recognition of $tRNA^{Cys}$. The $C_{277-461}$ fragment was tested separately for its ability to bind and discriminate $tRNA^{Cys}$. Previous studies showed that full-length $CysRS_{1-461}$ exhibited a specific fluorescence quenching upon binding of $tRNA^{Cys}$, using the strong intrinsic tryptophan fluorescence as a spectral probe (*23*). A titration of $tRNA^{Cys}$ concentrations revealed an equilibrium K_d of 0.33 μM (Figure 3) (*23*), which reflects the binding affinity of the CysRS−tRNA binary complex. Upon addition of a cysteinyl adenylate analogue, the K_d of the binary complex is increased to 1.7 μM, an indication of conformational changes in the CysRS−tRNA complex (*23*). Because of the sensitivity of the fluorescence titration to conformational changes in the complex, and because of its ability to assess binding under true equilibrium conditions without physically isolating the complex, this offers the best method for determining equilibrium binding affinity. Other methods, such as a gel shift or nitrocellulose binding assay, must isolate the complex by physical means

that can disrupt equilibrium. Thus, using the fluorescence titration, the $C_{277-461}$ fragment was examined for its binding affinity for $tRNA^{Cys}$ based on quenching of intrinsic tryptophan. The K_d for $tRNA^{Cys}$ was also found to be 0.33 μM, which suggested that key residues that contribute to tRNA binding are all located in the $C_{277-461}$ fragment. Importantly, both full-length $CysRS_{1-461}$ and the $C_{277-461}$ fragment were sensitive to substitutions of the tRNA anticodon. Mutations of the GCA anticodon to CUA increased the K_d to 5.2 μM for full-length CysRS and to 3.7 μM for the $C_{277-461}$ fragment. The similar effect on K_d emphasizes the dominance of the anticodon, and the recapitulation of the fragment in the overall binding capacity for tRNA.

The N_{1-287} fragment was also tested for tRNA binding by the fluorescence method. The ability of this fragment to weakly aminoacylate $microhelix^{Cys}$ suggested at least some affinity for the tRNA acceptor end. Indeed, fluorescence titration revealed a saturable binding curve, with a K_d of 9.5 μM for full-length $tRNA^{Cys}$ (Figure 3). This indicated a 30-fold reduced affinity compared to that of the full-length enzyme for the tRNA. The specificity of binding was then probed with the G73 variant of $tRNA^{Cys}$. While the full-length enzyme showed an almost 10-fold increase in K_d (to 2.5 μM), the N_{1-287} fragment showed little change (K_d = 7.2 μM, Figure 3). Thus, although U73 is the major determinant for aminoacylation for both the full-length protein and the N_{1-287} fragment, it is specifically recognized at the binding step only by the full-length enzyme, but not by the N_{1-287} fragment.

DISCUSSION

The N- and C-Terminal Fragments of E. coli CysRS Function Separately. On the basis of crystal structures of *E. coli* CysRS, we have dissected the enzyme into the N_{1-287} and $C_{277-461}$ fragments that contain the active site and anticodon-binding domains, respectively. The N_{1-287} fragment is comparable to the full-length enzyme in the activity for synthesis of cysteinyl adenylate, and for aminoacylation of the microhelix of $tRNA^{Cys}$. The $C_{277-461}$ fragment is active in tRNA binding, and accounts for the anticodon-dependent major binding interactions of the full-length enzyme. The ability of the N_{1-287} and $C_{277-461}$ fragments to each perform the expected functions in nearly full capacity validates the design of the dissection, and argues against the possibility of grossly misfolded proteins. These two fragments therefore provide a functional framework for addressing the mechanism and pathways of domain−domain communication.

Evidence for domain−domain communication is observed from comparison of the N_{1-287} fragment and CysRS in three aspects of the aminoacylation reaction. First, although the fragment has an efficiency of aminoacylation of $microhelix^{Cys}$ comparable to that of CysRS, its efficiency of aminoacylation of full-length tRNA is reduced by 10^6-fold (Figure 2 and Table 3). Second, although the fragment maintains the same specificity of aminoacylation of the microhelix as CysRS, its specificity with respect to full-length tRNA is reduced by 10^3-10^4-fold (Figure 2). Third, although the N_{1-287} fragment is capable of binding $tRNA^{Cys}$, it does not recognize U73 at the binding step, which is in clear contrast to the discriminating ability of CysRS at U73 (Figure 3). Together, these illustrate the deficiency of the N-terminal fragment in the efficiency and specificity of aminoacylation, and in recognition of tRNA for binding. The ability of the C-terminal domain in the full-length CysRS to strengthen these deficiencies suggests a communication between the two domains. The directionality of the communication can be evaluated also. Because the $C_{277-461}$ fragment has maintained both the capacity and specificity of tRNA binding of full-length CysRS, it itself is a functional entity, independent of the N-terminal fragment. This suggests that the signal of communication is transmitted from the anticodon-binding domain to the N-terminal catalytic domain.

Domain−Domain Communication Requires Covalent Continuity of both $tRNA^{Cys}$ and CysRS. Previous studies show that domain−domain communication for aminoacylation of tRNA with cysteine requires covalent continuity of the tRNA backbone (*21*). These studies were performed with the intact CysRS such that the acceptor and anticodon helices of $tRNA^{Cys}$ can be viewed as noncovalently "aligned" on the enzyme. The catalytic efficiency of aminoacylation was severely reduced, but was the same as that of the acceptor helix alone, suggesting no domain−domain communication. Here with the intact $tRNA^{Cys}$, the N_{1-287} and $C_{277-461}$ fragments of CysRS were noncovalently aligned on the tRNA, which still failed to show improvement of aminoacylation efficiency over that of the N_{1-287} fragment alone, indicating the absence of communication. Thus, the covalent connectivity of both $tRNA^{Cys}$ and CysRS is necessary for efficient domain−domain communication. The implication is that both molecules must be directly engaged in propagating signals of communication through intramolecular pathways. If the backbone of one molecule is broken, even with the other intact, the communication is interrupted. The requirement for the integrity of both molecules also suggests that, even though CysRS and tRNA make extensive contacts for aminoacylation, these intermolecular contacts do not provide the passage for domain−domain communication.

The kinetics of aminoacylation of the noncovalently assembled N_{1-287} and $C_{277-461}$ fragments provides new insights into the mechanism of communication (Table 3). While the K_m for $tRNA^{Cys}$ by the N_{1-287} fragment alone is increased from the normal value by >100-fold, the K_m in the reaction catalyzed by the two fragments is nearly normal. This suggests that the two fragments have complemented each other in approaching the tRNA for aminoacylation. The failure to achieve the catalytic efficiency of the intact CysRS therefore is due to the weak k_{cat}. The impaired k_{cat} suggests that, despite the overall correct alignment of the two fragments on $tRNA^{Cys}$ that restores the K_m, the catalytic residues in the active site and near the 3′ end of tRNA are not properly constrained for catalysis.

The crystal structure of *E. coli* CysRS, with and without $tRNA^{Cys}$, shed light on the enzyme conformation near the 3′ end of tRNA (*23*, *31*). In the complex, both the enzyme and tRNA make significant conformational changes in an induced-fit adaptation of each other. The enzyme reorganizes a large portion of the C-terminus that is disordered in the tRNA-free form into a mixed α/β fold that specifically recognizes the GCA anticodon of $tRNA^{Cys}$. The D-anticodon stem of $tRNA^{Cys}$ in turn bends sharply in its sugar−phosphate backbone to complement the shape of the enzyme, while the enzyme contacts the tRNA tertiary core to further discriminate on the basis of the shape of the tRNA backbone.

At the 3′ end of tRNA, the UCCA sequence forms a hairpin that curves into the active site of CysRS, while a large surface loop of the enzyme becomes ordered to stabilize the UCCA hairpin. The extensive mutual changes of the enzyme and tRNA support the notion that both need to be covalently intact to exert the required conformational changes.

Interestingly, the UCCA hairpin in the binary complex of the CysRS−$tRNA^{Cys}$ complex is in an unproductive conformation that occupies the ATP-binding site (*23*). This unproductive conformation provides a rationale for k_{cat} being the major determinant in domain−domain communication. Even with proper contacts between the enzyme and tRNA anticodon, the active site domain is in an unproductive conformation. Addition of the adenylate analogue Cys-AMS {5′-*O*-[*N*-(L-cysteinyl)sulfamoyl]adenosine} to the binary complex induces further conformation changes, which is indicated by a shift of the equilibrium binding constant for tRNA (*23*). These changes must occur at the active site near the 3′ end of tRNA to remove the unproductive conformation and prepare both molecules for catalysis. All of these changes require that both the enzyme and tRNA be in constant domain−domain communication to improve k_{cat}, and that this communication remain active until the completion of aminoacylation.

The Energetic Costs of Domain−Domain Communication. Previous studies have estimated that the energetic costs associated with communication within *E. coli* $tRNA^{fMet}$ between the acceptor and anticodon helices are quite large (∼7 kcal/mol) (*9*). A similar method is used to evaluate the energetic costs for the domain−domain communication between the N_{1-287} and $C_{277-461}$ fragments of CysRS. This is achieved by comparing the sum of free energy of binding of each fragment to $tRNA^{Cys}$ with the separately determined binding energy of the full-length CysRS. On the basis of the K_d values reported in Figure 3, the free energy of binding ($\Delta G°$) is calculated as $RT \ln K_d$, where R is the gas constant and T is the absolute temperature. After correction for the cratic entropy contribution ($-RT \ln 55 = -2.4$ kcal/mol), the $\Delta G°$ for the N_{1-287} fragment binding to $tRNA^{Cys}$ is −9.2 kcal/mol, the $\Delta G°$ for the $C_{277-461}$ fragment is −11.3 kcal/mol, and the $\Delta G°$ for full-length $CysRS_{1-461}$ is −11.3 kcal/mol. Thus, the sum of free energies for the two fragments is −20.5 kcal/mol, which is greater than the free energy of binding of CysRS by ∼9 kcal/mol. This suggests that approximately 9 kcal/mol of the sum of binding energies is used to link the two fragments together. Because of the possibility of new contacts with $tRNA^{Cys}$ upon alignment of the two fragments, the actual excess energy may be greater than 9 kcal/mol. Overall, the binding energies required for linking the synthetase fragments (9 kcal/mol) are similar to those required for joining the two domains in $tRNA^{fMet}$ (7 kcal/mol) (*9*).

Because synthetases often use binding energies to reduce the activation energy (*33*), it is of interest to also evaluate the difference in activation energy between the N_{1-287} fragment and full-length CysRS. This difference is estimated on the basis of the k_{cat}/K_m values reported in Table 3 {$-RT \ln[(2.1 \times 10^6)/(1.3 \times 10^2)]$}, which is approximately 6.1 kcal/mol. However, the difference in binding energy between the N_{1-287} fragment and CysRS is only 2.0 kcal/mol (see above). Even if the binding energy of the N-fragment is completely used for activation, there is a deficiency of approximately 4 kcal/mol that must be overcome. Thus, at least part or all of the excess binding energies (9.0 kcal/mol) generated by linking the two fragments together can pay for the energetic difference required to improve the catalytic efficiency of the N_{1-287} fragment to that of the full-length enzyme. This energetic cost must be used to constrain the catalytic site of the N_{1-287} fragment, to reorient the tRNA CCA end away from the ATP site, and to position it for catalysis. All of these rearrangements must be dedicated to improving the k_{cat} of aminoacylation. This study reveals that the utilization of binding energies for activation energy during the transition state of aminoacylation is only possible in the covalently linked CysRS. When the continuity of the enzyme is broken, the binding energies of the separated domains cannot be converted to activation energy.

Insights into the Naturally Split Synthetases. The high energetic costs required for domain−domain communication raise the question of how split synthetases can function with sufficient efficiency of aminoacylation in vivo. As shown here, the catalytic efficiency of CysRS is decreased by 10^4-fold upon splitting the enzyme into the N_{1-287} and $C_{277-461}$ fragments. Although the N_{1-287} fragment alone is sufficient to sustain cell viability, the growth rate is severely retarded (Table 2). Because the catalytic efficiency of the N_{1-287} and $C_{277-461}$ fragments together is similar to that of the N_{1-287} fragment alone, the growth rate supported by expression of the two fragments in vivo is likely to be retarded as well. It should be noted that the cellular environments contain abundant EF-Tu molecules and there is a high demand for rapid turnover of aminoacyl-tRNA for protein synthesis, both of which can enhance cellular rates of aminoacylation. However, these enhancements are unlikely to increase the catalytic efficiency of noncovalently assembled split synthetases by several orders of magnitude. The study here thus prompted further inspection of the naturally split synthetases. Only two split synthetase genes, the AlaRS gene encoded by the genome of the small obligate symbiont archaeon *Nanoarchaeum equitans* (*14*) and the LeuRS gene encoded by the hyperthermophilic bacteria *Aquifex aeolicus* (*15*), separate the synthetases on the basis of the division of the catalytic and tRNA-binding domains. Other split synthetases separate out the editing domain from the basic structure of synthetases. These include the PrdX protein of *Clostridium sticklandii* that catalyzes editing of Ala-$tRNA^{Pro}$ (*34*) and the Ybak protein of *H. influenzae* that removes Cys-$tRNA^{Pro}$ (*18*). The third type of split synthetases consists of activation domains of synthetases that have acquired new functions. These include the *E. coli* YadB protein, a paralog of the activation domain of GluRS that transfers the activated glutamate to the wobble position of $tRNA^{Asp}$ (*16*, *17*), the *E. coli* HisZ protein, a paralog of the activation domain of HisRS that is important for histidine biosynthesis (*35*), and the *Mycobacteria* MshC protein that is a paralog of CysRS but is involved in the biosynthesis of mycothiol (*32*).

AlaRS and LeuRS are unique in that efficient aminoacylation of tRNA depends primarily on the acceptor stem. The major determinant for aminoacylation with alanine is a G3·U70 base pair in the acceptor stem (*36*, *37*), while those for aminoacylation with leucine by bacterial LeuRS are the A73 base of the acceptor stem and nucleotides in the tRNA tertiary core (*38*, *39*). In both cases, the anticodon is not important and thus does not require a strong domain−domain

communication with the acceptor end. Indeed, the *E. coli* LeuRS has been artificially split in the editing domain, and most of the split proteins have retained at least 10% of the activity of the native protein (*40*). There is only one split protein that has ~1% of the activity of native LeuRS, but even this activity is 100−1000-fold higher than the 10^4-fold decreased activity of the split CysRS reported here. This emphasizes that for AlaRS and LeuRS, the existence of naturally split proteins arises from the lack of a strong requirement for domain−domain communication between the active site and the anticodon-binding site. The identification of isolated editing domains suggests that, while editing is important for the fidelity of aminoacylation, it can be achieved without a covalent linkage to the catalytic or tRNA-binding domain. Indeed, the editing catalyzed by the isolated editing domain is to hydrolyze the incorrect amino acids that have been transferred to tRNA in the form of aminoacyl-tRNAs, which in principle can be recognized by separate protein molecules without direct communication with the active site domain. Finally, the paralogs of synthetases constitute a new class of enzymes that catalyze transfer between small molecules without a need for long-range communication. For example, HisZ transfers ATP to phosphoribosyl pyrophosphate, while MshC transfers cysteinyl adenylate to glucopyranoside inositol. Although the acceptor of YadB is $tRNA^{Asp}$, the site of transfer is the wobble base of the anticodon but not the 3′ end of tRNA (*16*, *17*). In these synthetase paralogs, the active site that activates the donor is likely to also accommodate the acceptor. Even if some communication is required between the active site domain and the acceptor-binding domain, the energetic costs of communication between domains are probably small and can be afforded in cellular environments. This analysis provides new insights into the concept of split genes, and emphasizes that the split can take place only when long-range domain−domain communication is not required.

ACKNOWLEDGMENT

We thank members of our laboratory for discussion, and two anonymous reviewers for their comments.

REFERENCES

1. Ibba, M., and Soll, D. (2000) Aminoacyl-Trna Synthesis, *Annu. Rev. Biochem. 69*, 617−650.
2. Schimmel, P., Giege, R., Moras, D., and Yokoyama, S. (1993) An operational RNA code for amino acids and possible relationship to genetic code, *Proc. Natl. Acad. Sci. U.S.A. 90*, 8763−8768.
3. Alexander, R. W., and Schimmel, P. (2001) Domain-domain communication in aminoacyl-tRNA synthetases, *Prog. Nucleic Acid Res. Mol. Biol. 69*, 317−349.
4. Giege, R., Sissler, M., and Florentz, C. (1998) Universal rules and idiosyncratic features in tRNA identity, *Nucleic Acids Res. 26*, 5017−5035.
5. Musier-Forsyth, K., and Schimmel, P. (1993) Aminoacylation of RNA oligonucleotides: Minimalist structures and origin of specificity, *FASEB J. 7*, 282−289.
6. Martinis, S. A., and Schimmel, P. (1995) in *tRNA: Structure, Biosynthesis, and Function* (Soll, D., and RajBhandary, U. L., Eds.) pp 390−370, The American Society of Microbiology Press, Washington, DC.
7. Alexander, R. W., Nordin, B. E., and Schimmel, P. (1998) Activation of microhelix charging by localized helix destabilization, *Proc. Natl. Acad. Sci. U.S.A. 95*, 12214−12219.
8. Frugier, M., Florentz, C., and Giege, R. (1992) Anticodon-independent aminoacylation of an RNA minihelix with valine, *Proc. Natl. Acad. Sci. U.S.A. 89*, 3990−3994.
9. Gale, A. J., Shi, J. P., and Schimmel, P. (1996) Evidence that specificity of microhelix charging by a class I tRNA synthetase occurs in the transition state of catalysis, *Biochemistry 35*, 608−615.
10. Kato, I., and Anfinsen, C. B. (1969) On the stabilization of ribonuclease S-protein by ribonuclease S-peptide, *J. Biol. Chem. 244*, 1004−1007.
11. Burbaum, J. J., and Schimmel, P. (1991) Assembly of a class I tRNA synthetase from products of an artificially split gene, *Biochemistry 30*, 319−324.
12. Shiba, K., and Schimmel, P. (1992) Tripartite functional assembly of a large class I aminoacyl tRNA synthetase, *J. Biol. Chem. 267*, 22703−22706.
13. Shiba, K., and Schimmel, P. (1992) Functional assembly of a randomly cleaved protein, *Proc. Natl. Acad. Sci. U.S.A. 89*, 1880−1884.
14. Waters, E., Hohn, M. J., Ahel, I., Graham, D. E., Adams, M. D., Barnstead, M., Beeson, K. Y., Bibbs, L., Bolanos, R., Keller, M., Kretz, K., Lin, X., Mathur, E., Ni, J., Podar, M., Richardson, T., Sutton, G. G., Simon, M., Soll, D., Stetter, K. O., Short, J. M., and Noordewier, M. (2003) The genome of *Nanoarchaeum equitans*: Insights into early archaeal evolution and derived parasitism, *Proc. Natl. Acad. Sci. U.S.A. 100*, 12984−12988.
15. Xu, M. G., Chen, J. F., Martin, F., Zhao, M. W., Eriani, G., and Wang, E. D. (2002) Leucyl-tRNA synthetase consisting of two subunits from hyperthermophilic bacteria *Aquifex aeolicus*, *J. Biol. Chem. 277*, 41590−41596.
16. Salazar, J. C., Ambrogelly, A., Crain, P. F., McCloskey, J. A., and Soll, D. (2004) A truncated aminoacyl-tRNA synthetase modifies RNA, *Proc. Natl. Acad. Sci. U.S.A. 101*, 7536−7541.
17. Dubois, D. Y., Blaise, M., Becker, H. D., Campanacci, V., Keith, G., Giege, R., Cambillau, C., Lapointe, J., and Kern, D. (2004) An aminoacyl-tRNA synthetase-like protein encoded by the *Escherichia coli* yadB gene glutamylates specifically tRNAAsp, *Proc. Natl. Acad. Sci. U.S.A. 101*, 7530−7535.
18. An, S., and Musier-Forsyth, K. (2004) Trans-editing of Cys-tRNAPro by *Haemophilus influenzae* YbaK protein, *J. Biol. Chem. 279*, 42359−42362.
19. Hou, Y. M., Shiba, K., Mottes, C., and Schimmel, P. (1991) Sequence determination and modeling of structural motifs for the smallest monomeric aminoacyl-tRNA synthetase, *Proc. Natl. Acad. Sci. U.S.A. 88*, 976−980.
20. Komatsoulis, G. A., and Abelson, J. (1993) Recognition of tRNA(Cys) by *Escherichia coli* cysteinyl-tRNA synthetase, *Biochemistry 32*, 7435−7444 [erratum: (1993) *Biochemistry 32*, 13374].
21. Hamann, C. S., and Hou, Y. M. (1995) Enzymatic aminoacylation of tRNA acceptor stem helices with cysteine is dependent on a single nucleotide, *Biochemistry 34*, 6527−6532.
22. Hou, Y. M., Motegi, H., Lipman, R. S., Hamann, C. S., and Shiba, K. (1999) Conservation of a tRNA core for aminoacylation, *Nucleic Acids Res. 27*, 4743−4750.
23. Hauenstein, S., Zhang, C. M., Hou, Y. M., and Perona, J. J. (2004) Shape-selective RNA recognition by cysteinyl-tRNA synthetase, *Nat. Struct. Mol. Biol. 11*, 1134−1141.
24. Zhang, C. M., Christian, T., Newberry, K. J., Perona, J. J., and Hou, Y. M. (2003) Zinc-mediated Amino Acid Discrimination in Cysteinyl-tRNA Synthetase, *J. Mol. Biol. 327*, 911−917.
25. Fersht, A. R., Ashford, J. S., Bruton, C. J., Jakes, R., Koch, G. L., and Hartley, B. S. (1975) Active site titration and aminoacyl adenylate binding stoichiometry of aminoacyl-tRNA synthetases, *Biochemistry 14*, 1−4.
26. Hou, Y. M., Westhof, E., and Giege, R. (1993) An unusual RNA tertiary interaction has a role for the specific aminoacylation of a transfer RNA, *Proc. Natl. Acad. Sci. U.S.A. 90*, 6776−6780.
27. Zhang, C. M., Perona, J. J., and Hou, Y. M. (2003) Amino acid discrimination by a highly differentiated metal center of an aminoacyl-tRNA synthetase, *Biochemistry 42*, 10931−10937.
28. Hou, Y. M., Sundaram, M., Zhang, X., Holland, J. A., and Davis, D. R. (2000) Recognition of functional groups in an RNA helix by a class I tRNA synthetase, *RNA 6*, 922−927.
29. Hou, Y. M., Zhang, X., Holland, J. A., and Davis, D. R. (2001) An important 2′-OH group for an RNA-protein interaction, *Nucleic Acids Res. 29*, 976−985.
30. Zhang, C., and Hou, Y. (2004) Synthesis of cysteinyl-tRNACys by a prolyl-tRNA synthetase, *RNA Biol. 1*, 35−41.

31. Newberry, K. J., Hou, Y. M., and Perona, J. J. (2002) Structural origins of amino acid selection without editing by cysteinyl-tRNA synthetase, *EMBO J. 21*, 2778−2787.
32. Sareen, D., Steffek, M., Newton, G. L., and Fahey, R. C. (2002) ATP-dependent L-cysteine:1D-myo-inosityl 2-amino-2-deoxy-α-D-glucopyranoside ligase, mycothiol biosynthesis enzyme MshC, is related to class I cysteinyl-tRNA synthetases, *Biochemistry 41*, 6885−6890.
33. Wells, T. N., and Fersht, A. R. (1986) Use of binding energy in catalysis analyzed by mutagenesis of the tyrosyl-tRNA synthetase, *Biochemistry 25*, 1881−1886.
34. Ahel, I., Korencic, D., Ibba, M., and Soll, D. (2003) Trans-editing of mischarged tRNAs, *Proc. Natl. Acad. Sci. U.S.A. 100*, 15422−15427.
35. Sissler, M., Delorme, C., Bond, J., Ehrlich, S. D., Renault, P., and Francklyn, C. (1999) An aminoacyl-tRNA synthetase paralog with a catalytic role in histidine biosynthesis, *Proc. Natl. Acad. Sci. U.S.A. 96*, 8985−8990.
36. Hou, Y. M., and Schimmel, P. (1988) A simple structural feature is a major determinant of the identity of a transfer RNA, *Nature 333*, 140−145.
37. Francklyn, C., and Schimmel, P. (1990) Enzymatic aminoacylation of an eight-base-pair microhelix with histidine, *Proc. Natl. Acad. Sci. U.S.A. 87*, 8655−8659.
38. Tocchini-Valentini, G., Saks, M. E., and Abelson, J. (2000) tRNA leucine identity and recognition sets, *J. Mol. Biol. 298*, 779−793.
39. Du, X., and Wang, E. D. (2003) Tertiary structure base pairs between D- and TpsiC-loops of *Escherichia coli* tRNA(Leu) play important roles in both aminoacylation and editing, *Nucleic Acids Res. 31*, 2865−2872.
40. Li, T., Guo, N., Xia, X., Wang, E. D., and Wang, Y. L. (1999) The peptide bond between E292-A293 of *Escherichia coli* leucyl-tRNA synthetase is essential for its activity, *Biochemistry 38*, 13063−13069.

BI050285Y